THE KINETICS OF LOCAL ANESTHETIC BLOCKADE OF END-PLATE CHANNELS

ROBERT L. RUFF
Department of Physiology and Biophysics, and Medicine (Neurology), SJ-40, University of Washington, Seattle, Washington 98195

ABSTRACT The effect of the local anesthetic QX222 on the kinetics of miniature end-plate currents (MEPC) and acetylcholine-induced end-plate current fluctuations was studied in voltage-clamped frog cutaneous pectoris neuromuscular junctions. The rate constants for a kinetic scheme of local anesthetic blockage of end-plate channels were calculated from the MEPC decay parameters. At 18°C the blocking rate constant was $1.1 \pm 0.3 \times 10^7$ exp $(-0.009 \pm 0.003 \times V)$ $s^{-1}M^{-1}$, and the unblocking rate constant was $5.7 \pm 0.6 \times 10^2$ exp $(0.011 \pm 0.002 \times V)$ s^{-1}. The dissociation constant was close to 10 μM at -80 mV. End-plate fluctuations indicated that the local anesthetic QX222 lowered the effective single-channel conductance, suggesting a finite blocked state conductance that was calculated to be 1.6 pS. The apparent differences between QX222 interaction with end-plate and extrajunctional channels are discussed.

INTRODUCTION

End-plate currents (EPC) and miniature end-plate currents (MEPC) normally decay with a single exponential time-course (1–9) that may be represented as

$$I(t) = I_0 e^{-\alpha t}, \qquad (1)$$

where $I(t)$ is the current, I_0 is the amplitude and α is the decay rate. Individual end-plate channels contribute a square pulse of current (10). The exponential decay of normal EPC and MEPC reflects the distribution mean open times of the end-plate channels (11). In the presence of local anesthetics, EPC and MEPC decay with time-courses that can be described by the sum of two exponential decays (8, 9, 12–17):

$$I(t) = I_1 e^{-k_1 t} + I_2 e^{-k_1 t}, \qquad (2)$$

where $k_2 > \alpha > k_1$. Hyperpolarization or increase in local anesthetic concentration increases k_2 and I_2/I_1, and decreases k_1 (8, 9, 17).

Analysis of EPC fluctuations (8, 9) and voltage-jump studies of EPC (18) suggested that local anesthetics enter and block open end-plate channels. Neher and Steinbach (19) directly demonstrated that local anesthetic molecules reversibly block open extrajunctional channels. This kinetic scheme of local anesthetic action may be represented as:

$$nT + R \rightleftharpoons TnR \underset{\alpha}{\overset{\beta}{\rightleftharpoons}} TnR^* + Q \underset{F}{\overset{G}{\rightleftharpoons}} TnR^*Q, \qquad (3)$$

where T represents transmitter, R is the acetylcholine receptor (AChR), Q is the local anesthetic molecule, TnR^* is the open configuration of the channel and TnR^*Q is the blocked configuration. According to this scheme the rapid phase of the EPC decay occurs because an open channel can transfer to a lower conductance state by transition to the blocked state as well as by channel closure. The slow component of the EPC results because blocked channels are unable to close until they transfer back to the open configuration.

Lewis and Stevens (20, 21) and Hille et al. (22, 23) have provided strong evidence that the end-plate channel is a cationic permeant pore that contains specific binding sites for ions such as local anesthetic molecules. By accurately measuring the voltage dependence of G and F, the blocking and unblocking rate constants for local anesthetic molecules, one can characterize the location of the local anesthetic binding site within the end-plate channel, and the affinity of local anesthetics for this binding site. Thus, analysis of the voltage dependence of local anesthetic action can provide information on the electrical structure of the end-plate channels.

Neher and Steinbach (19) measured the blocking and unblocking rate constants for two lidocaine derivatives (QX222 and QX314) at extrajunctional receptors using suberyldicholine (SubCh) as the agonist. Adams (18) studied the voltage sensitivity of procaine blockade of end-plate channels activated by SubCh. From these rate constants they calculated the equilibrium dissociation constant of the local anesthetic-channel complex and the location of the local anesthetic binding site within the extrajunctional and end-plate channels.

The channels associated with extrajunctional AChR have a longer mean open time and smaller conductance than end-plate channels (24–26). In addition, the mean

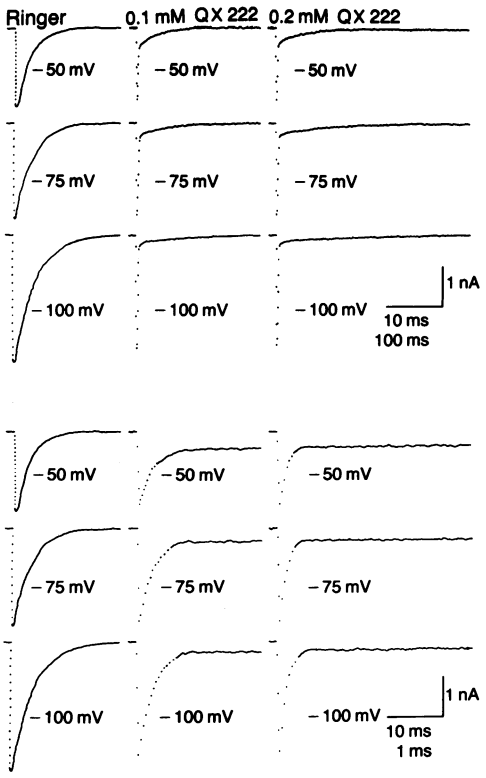

FIGURE 1 QX222 produces a biphasic MEPC decay. Each trace is an average of 10–15 MEPC. In Ringer solution hyperpolarization slows the single exponential decay rate. With QX222 present, increased local anesthetic concentration or hyperpolarization results in the slow phase becoming slower, the rapid phase faster, and the relative amplitude of the rapid phase increases (see also Fig. 2). Time calibration: Ringer solution, 10 ms; QX222 upper traces, 100 ms; lower traces, 1 ms.

open time of channels activated by SubCh is longer than of those activated by acetylcholine (ACh) (25, 27). Therefore, the kinetics of local anesthetic action on extrajunctional receptors or end-plate channels activated by SubCh may be different from that found at the end-plate with the naturally occurring agonist, ACh.

In this study, I determined the apparent blocking and unblocking rate constants of QX222 for end-plate channels activated by ACh and found them qualitatively similar to those previously observed at extrajunctional and end-plate channels. The rate constants were less voltage-dependent than those found for extrajunctional receptors, which suggests that the local anesthetic binding site is closer to the outside surface in end-plate channels compared with extrajunctional channels. The conductance of the blocked state was estimated from the apparent single channel conductance measured before and after applying QX222.

METHODS

MEPC and EPC current fluctuations recorded from the m. cutaneous pectoris of *Rana pipiens* were studied in frog Ringer solutions which contained 0, 0.1-, and 0.2-mM QX222 (Astra). 23 cells from 13 preparations were studied. Except as indicated below, the details of the data recording and analysis were unchanged from a previous description (9). All studies were carried out at 18° ± 1°C. The sampling interval for EPC current fluctuations was 0.5 ms for 13 cells. In 10 cells EPC current fluctuations were obtained at 0.5, 0.25, 0.1, 0.05, and 0.025 ms sampling intervals with corresponding low-pass filter (Butterworth) settings of 1, 2, 5, 10, and 20 kHz. The EPC variance was calculated by integrating the power spectra. Cells were studied at holding potentials ranging from −50 to −100 mV in 5-mV increments. Values are recorded as mean ± SD.

RESULTS

MEPC recorded in Ringer solution decayed with a single exponential time-course in the form of Eq. 1 (Fig. 1). In the presence of the local anesthetic QX222, the MEPC had complex decays with rapid and slow decay rates in the form of Eq. 2 (Fig. 1). The MEPC decay rates determined according to Eqs. 1 and 2 are shown in Fig. 2.

The kinetic scheme for local anesthetic action shown in Eq. 3 predicts MEPC in the form of Eq. 2 with

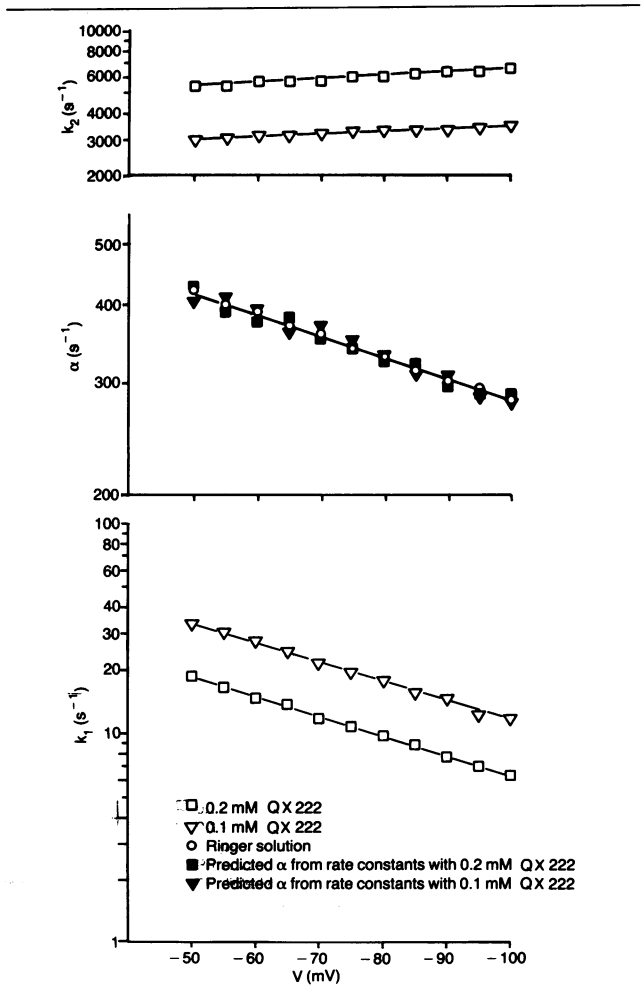

FIGURE 2 The voltage dependence of the MEPC decay rates in Ringer solution, 0.1- and 0.2-mM QX222 for the cell shown in Fig. 1. The observed decay rates (open figures) were obtained from decomposition of the MEPC in the form of Eqs. 1 and 2. The predicted decay rates (closed figures) were calculated from Eq. 8. The solid lines are least-square fits.

$$k_1 = \{\alpha + F + G \cdot C_Q - [(\alpha + F + G \cdot C_Q)^2 - 4\alpha \cdot F]^{1/2}\}/2 \quad (4)$$

$$k_2 = \{\alpha + F + G \cdot C_Q + [(\alpha + F + G \cdot C_Q)^2 - 4\alpha \cdot F]^{1/2}\}/2 \quad (5)$$

and

$$I_2/I_1 = (k_2 - F)/(F - k_1), \quad (6)$$

where C_Q is the local anesthetic concentration (9, 18, 25, 28). As shown in Fig. 2, k_1 decreases and k_2 increases with hyperpolarization or increased QX222 concentration as predicted by Eqs. 4 and 5. The rate constants in Eq. 3 can be described in terms of measurable MEPC parameters as:

$$F = [k_2 + k_1(I_2/I_1)]/(I_2/I_1 + 1) \quad (7)$$

$$\alpha = [k_2 k_1 (I_2/I_1 + 1)]/[k_2 + k_1(I_2/I_1)] \quad (8)$$

$$G \cdot C_Q = k_2 + k_1 - (\alpha + F). \quad (9)$$

QX222 Does not Effect Channel Closure

According to Eq. 3 the transition from the open to the closed state should not be affected by local anesthetics. Therefore, α measured in the absence of QX222 (Eq. 1) should be the same as that determined by Eq. 8 when QX222 is present. Fig. 2 shows that the values of α measured in Ringer solution agreed closely with those determined when the same cell was studied with QX222 in the bath. In the 23 cells studied, the MEPC decay rates measured before applying QX222 were within 8% of the calculated rate constant, α, with QX222 present.

Binding and Unbinding Rate Constants

The rate constants F and $G \cdot C_Q$ calculated by Eqs. 7 and 9, varied with the membrane voltage and concentration of QX222 in the manner predicted by Eq. 3 (Fig. 3). The rate constant $G \cdot C_Q$ for blockade of the end-plate channel by the positively charged anesthetic molecule, increased with hyperpolarization, and was linearly proportional to the local anesthetic concentration. The rate constant for removal of the anesthetic molecule from the channel, F, increased with depolarization and was independent of QX222 concentration. Both G and F varied exponentially with voltage. Their average values were

$$G = 1.1 \pm 0.3 \times 10^7 \exp(-0.009 \pm 0.003 \times V) \quad (10)$$

$$F = 5.7 \pm 0.6 \times 10^2 \exp(0.011 \pm 0.002 \times V) \quad (11)$$

where G is in $s^{-1}M^{-1}$, F is in s^{-1}, V the membrane voltage is in millivolts, and $n = 46$.

The equilibrium dissociation constant for end-plate channel blocking was

$$K_D = F/G = 5.2 \times 10^{-5} \exp(0.02 \times V),$$

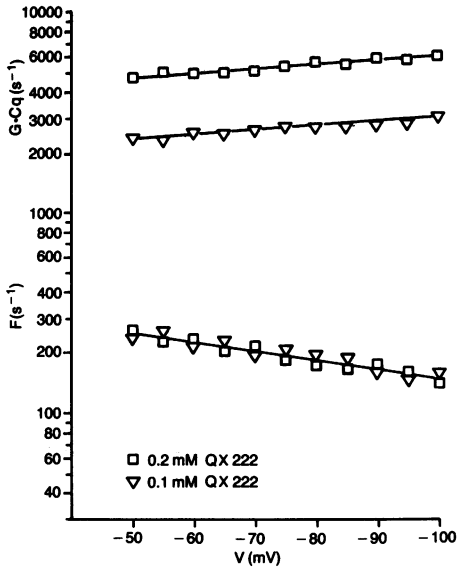

FIGURE 3 The calculated rate constant for end-plate blockade, $G \cdot C_Q$, increased exponentially with hyperpolarization and increased linearly with local anesthetic concentration. The unblocking rate constant, F, decreased exponentially with hyperpolarization and did not vary with local anesthetic concentration. The rate constants were obtained using Eqs. 7 and 9 for the cell shown in Figs. 1 and 2. The solid lines are least-square fits.

where K_D is in M. At -80 mV a value close to 10 μM is obtained.

Conductance of the Blocked State

The single-channel conductance γ can be calculated as (5)

$$\gamma = \sigma^2/(\mu_I[V - V_{eq}]) \quad (12)$$

where σ^2 is the EPC variance, μ_I is the mean EPC, and V_{eq} is the equilibrium potential. In Ringer solution $\gamma = 26.1 \pm 1.6$ pS ($n = 253$), and did not vary with membrane potential. For the blocking scheme of local anesthetic action (Eq. 3) the single-channel conductance $\bar{\gamma}$, is a mean of the conductance of the open state γ_1, and the blocked state γ_2, which is weighted according to the probability that the channel will be in these states:

$$\bar{\gamma} = (\gamma_1^2 P_1 + \gamma_2^2 P_2)/(\gamma_1 P_1 + \gamma_2 P_2), \quad (13)$$

where P_1 is the unconditional probability that a channel is open, and P_2 is the unconditional probability that a channel is blocked (9). In deriving Eq. 13, it was assumed that the probability of the channel being in an open or blocked state was small. For the kinetic scheme in Eq. 3, $P_2/P_1 = (G \cdot C_Q)/F$.

Therefore, provided that γ_1 and γ_2 are constant and $\gamma_1 > \gamma_2 > 0$, Eq. 13 predicts that $\bar{\gamma}$ should decrease with hyperpolarization or with increases in QX222 concentration. Fig. 4 illustrates that $\bar{\gamma}$ varies with voltage and concentration of QX222 as predicted by Eq. 13. Assuming

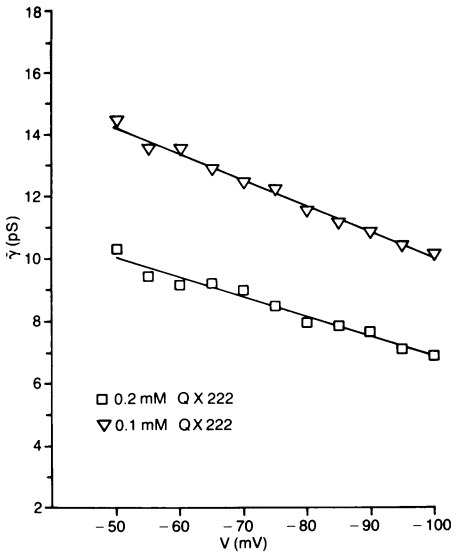

FIGURE 4 The effective single channel conductance, $\bar{\gamma}$, decreased with increased QX222 concentration, and hyperpolarization. These values are for the same cell shown in Figs. 1–3. The single channel conductance for this cell in Ringer solution is 24.6 pS. The solid lines are obtained from Eq. 13 with γ_1 = 24.6 pS and γ_2 = 1.8 pS.

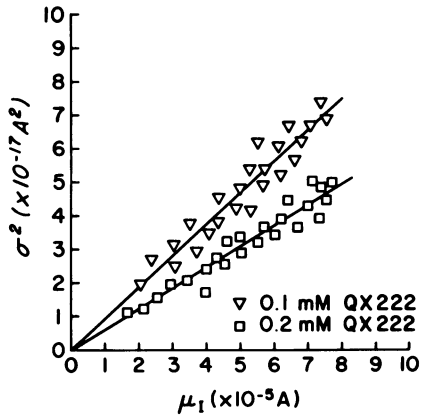

FIGURE 5 The EPC variance, σ^2, increased linearly with the iontophoretically-induced mean EPC, μ_I. The data is from 13 cells studied at −75 mV. The solid lines are least-square linear regression fits, which yield according to Eq. 12, γ = 12.6 pS in 0.1-mM QX222 and γ = 8.5 pS in 0.2-mM QX222.

that γ_1 is not changed by QX222, it is possible to calculate γ_2 according to Eq. 13, using the values of F and $G \cdot C_Q$ calculated by Eqs. 7 and 9, and equating γ_1 with the single-channel conductance measured in Ringer solution. The conductance of the blocked state did not vary appreciably with membrane voltage or local anesthetic concentration. The average value was: γ_2 = 1.62 ± 0.21 pS (n = 506).

Reduction in $\bar{\gamma}$ Is Not Due to a Reduction in the Number of Available End-Plate Channels

Adams (18) has suggested that the decrease in single-channel conductance found with QX222 (9) might result if the fraction of channels that are open (blocked or unblocked) with local anesthetic present is not a small proportion of the total number of available channels. According to this proposal the kinetics of the ACh-AChR interaction would no longer be Poisson, and the slope of σ vs. μ_I would decrease at higher values of μ_I (6). However, σ remained proportional to μ_I over a range of agonist concentrations used in this study (Fig. 5), which suggests that the change in γ did not result from a reduction in the population of end-plate channels that can open.

Reduction in $\bar{\gamma}$ Is Not an Artifact of Filtering

Because the local anesthetic decreases the mean open time of the end-plate channels, the reduction in single-channel conductance could be an artifact of filtering. In this case, $\bar{\gamma}$ would be reduced because filtering attenuated the unitary EPC of the open and unblocked channel. The measured single-channel conductance would appear to be lower because of an artifactual lowering of the open-channel conductance rather than a finite blocked state conductance. If filtering were responsible for the reduction in γ when local anesthetic is present, then $\bar{\gamma}$ should increase as the low pass filter frequency is increased. The relationship between γ and the filter setting was studied in 10 cells. For low-pass filter frequencies up to 20 kHz, $\bar{\gamma}$ did not vary with the filtering frequency (Fig. 6), which indicates that the reduction in $\bar{\gamma}$ was not an artifact of filtering.

DISCUSSION

The rate constants for a kinetic scheme of local anesthetic interaction with end-plate channels (Eq. 3) were calculated from MEPC parameters (Eqs. 7–9). The values

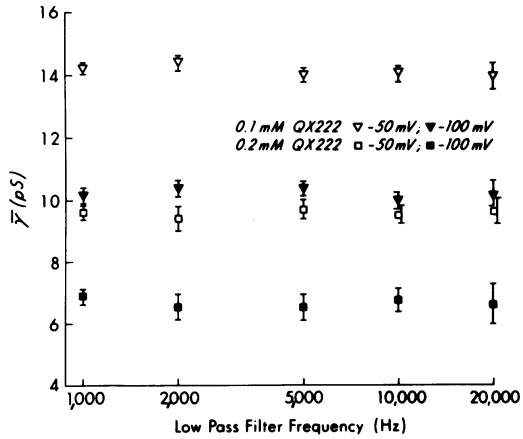

FIGURE 6 The effective single channel conductance, $\bar{\gamma}$, did not vary with the low-pass filtering frequency between 1 and 20 kHz. The data is from 10 cells. The error bars are ±1 SE.

obtained were consistent with this scheme in which a single local anesthetic molecule will reversibly block an open end-plate channel. As predicted, the channel closure rate was unaffected by the local anesthetic, the blocking rate increased with hyperpolarization and local anesthetic concentration, and the unblocking rate increased with depolarization and was independent of local anesthetic concentration. The close agreement between expected and calculated kinetic behavior provides additional support to the prior studies which indicated that local anesthetic molecules blocked end-plate channels (9, 18, 19). Neher and Steinbach (19) directly measured the rate constants for single extrajunctional channel closure and blockade, and found that they behaved in accordance with Eq. 3. Adams (18) calculated the rate constants for procaine blockade and removal from end-plate channels opened by SubCh, and also found them to be consistent with Eq. 3.

Validity of Assuming $\gamma_2 = 0$ in Kinetic Calculations

Eq. 6 was derived by assuming that $\gamma_2/\gamma_1 = 0$. The data indicates that $\gamma_2/\gamma_1 = 0.06$. By iteration one can calculate the values of G and F with $\gamma_2/\gamma_1 = 0.06$ (9). When this is done the calculated values of F and G are within 7% of the values obtained by assuming that the blocked state is nonconducting. Therefore, a small blocked-state conductance does not appreciably alter the calculation of the blocking and unblocking rate constants.

Other Schemes of Local Anesthetic Action

Steinbach (29) initially proposed that local anesthetics act at end-plate channels by causing a transition from the open state to a lower conductance state. Subsequently, several studies have suggested that local anesthetic molecules block end-plate channels (9, 18, 19). Rather than blocking the end-plate channels, the anesthetic could bind to the AChR and induce a conformation change to a lower conductance state. Adams (18) and Neher and Steinbach (19) have argued against this model. Redmann's observation (20) that sodium competes with QX222 for a binding site within the end-plate channel, and recent studies indicating that the end-plate channel is too small for QX222 to pass through (27, 28), add further support to the blocking scheme of local anesthetic action.

Using the results of equilibrium studies, Adams (18) has suggested that local anesthetics may slowly bind to closed end-plate channels. As discussed by Neher and Steinbach (19), transitions between the closed and blocked states which occur at a rate smaller than $\alpha/10$ would not be detected in kinetic studies. Such slow transitions would not appreciably change Eqs. 6–8. In their kinetic studies, Adams (18) and Neher and Steinbach (19) found no evidence for transitions between the closed and blocked states.

Comparison of G, and K_D with Previous Values

The value of the blocking rate constant at -80 mV found in this study, $G = 2.3 \times 10^7 M^{-1}s^{-1}$ agrees closely with the previous values for end-plate channels, $G = 2\text{–}2.3 \times 10^7 M^{-1}s^{-1}$ (18, 30), and extrajunctional channels, $1.2 \times 10^7 M^{-1}s^{-1}$ (19), activated by SubCh. The value of the dissociation constant, K_D, at -80 mV was 10 μM (5–25 μM range), compared with the previous values of 20 μM (18) and 40 μM (30) for end-plate channels, and 100 μM (19) for extrajunctional channels. Part of the discrepancy between the end-plate values may reflect the temperature dependence of K_D. Previous evidence suggested that K_D increased with temperature (9). The value of 40 μM was obtained at 21°–23°C, whereas the experiments reported here were performed at 18°C. The extrajunctional experiments were performed at 8°C, therefore temperature correction would widen the gap between the end-plate and extrajunctional values of K_D. The voltage dependence of K_D was also different for end-plate and extrajunctional channels. In this study, K_D changed e-fold per 50 mV; previous end-plate values for an e-fold change in K_D were 50–60 mV (18, 30), whereas the determination for extrajunctional receptors was 32 mV (19). This suggests a difference in the binding of local anesthetics to end-plate vs. extrajunctional channels.

Local Anesthetics Bind More Tightly to EPC than to Extrajunctional Channels

The zero-field values of the rate constants F and G indicate the affinity of the local anesthetic molecule for its binding site within the channel. Using a Q_{10} of 3 for k_1 and k_2 (17) and 1.2 for I_1/I_2 (unpublished observation), it is possible to calculate values for F and G at 8°C, and thus compare the values of the zero-field blocking and unblocking rate constants at end-plate channels with those measured at extrajunctional channels (19). The blocking rate constants are similar at end-plate ($G = 9.2 \times 10^6 s^{-1}M^{-1}$) and extrajunctional ($G = 3.8 \times 10^6 s^{-1}M^{-1}$) channels, whereas the unbinding rate constant is faster for extrajunctional channels ($F = 4.5 \times 10^3 s^{-1}$) than for end-plate channels ($F = 1.2 \times 10^2 s^{-1}$). The blocking rates are similar to the blocking rates for other drugs at end-plate channels (31–34), and for local anesthetics at other sites (35, 36). As suggested by Adams (18) and Neher and Steinbach (19) the blocking reaction could be diffusion controlled. The apparent difference between the local anesthetic unbinding rate constants for extrajunctional and end-plate channels may be due to the different techniques used to record the extrajunctional currents (19). Alternatively, the slower unbinding rate for the end-plate channels may indicate that the local anesthetic is more tightly bound to end-plate channels.

Location of the Binding Site

The voltage dependence of K_D suggests the location of the binding site within the channel (36). For a univalent cation binding within the channel,

$$K_D = K_{D,0} \exp(f \cdot e \cdot V/kT)$$

where e is the electronic charge, f is the fraction of the membrane field sensed by the ion as it reaches the binding site, and kT has the usual thermodynamic significance. For local anesthetics binding to end-plate channels $f = 0.5$ (18, 30) whereas $f = 0.78$ (19) for extrajunctional channels. Assuming a constant membrane field, the local anesthetic binding site is approximately halfway through the membrane for end-plate channels and three-quarters across the membrane in extrajunctional channels.

Conductance of the Blocked State

QX222 decreased the single-channel conductance. Katz and Miledi (38) reported that procaine reduced the single-channel conductance at the end-plate. My results suggest that the smaller single-channel conductance results from a finite conductance of the blocked state which is 6% of the open-state conductance. This is slightly larger than the 5% upper limit value reported for extrajunctional channels (19). In calculating $\bar{\gamma}$, the open-state conductance was assumed to be unchanged. The decreased single-channel conductance could alternatively have resulted from reduction of the open-state conductance. However, local anesthetics did not decrease the open-state conductance at extrajunctional channels (19). Inaccuracy in the calculations of F or G would produce an incorrect value for γ_2. The close agreement between the values of F and G in this study with the previous values suggest that these rate constants were not grossly inaccurate. However, if G/F was underestimated by a factor of 2, then γ_2 would be approximately 0.9 pS or 3.6% of the open-state conductance. Alternatively, the larger blocked state conductance in this study could result from a difference between end-plate and extrajunctional channels.

I wish to thank Drs. Stevens and Gardner for their support of this work, and Drs. Detwiler and Hille for their helpful comments on the manuscript.

This work was supported by National Institutes of Health grants 5-R01-NS12961 to Dr. Stevens and NIH grants 5-K07-NS00498 and 1-R01-NS16696 to Dr. Ruff, and U.S. Public Health Service grant NS11555 to Dr. Gardner.

Received for publication 23 April 1981 and in revised form 13 July 1981.

REFERENCES

1. Gage, P. W., and R. N. McBurney. 1972. Miniature end-plate currents and potentials generated by quanta of acetylcholine in glycerol-treated toad sartorius fibers. *J. Physiol. (Lond.)*. 226:79–94.
2. Kordas, M. 1972. An attempt at an analysis of the factors determining the time course of the end-plate current. I. The effects of prostigmine and of the ratio of Mg^{++} to Ca^{++}. *J. Physiol. (Lond.)*. 224:317–332.
3. Kordas, M. 1972. An attempt at an analysis of the factors determining the time course of the end-plate current. II. Temperature. *J. Physiol. (Lond.)*. 224:333–348.
4. Magleby, K. L. and C. F. Stevens. 1972. The effect of voltage on the time course of end-plate currents. *J. Physiol. (Lond.)*. 223:151–171.
5. Anderson, C. R. and C. F. Stevens. 1973. Voltage clamp analysis of acetylcholine produced end-plate current fluctuations at frog neuromuscular junction. *J. Physiol. (Lond.)*. 235:655–691.
6. Dionne, V. E., and C. F. Stevens. 1975. Voltage dependence of agonist effectiveness at the frog neuromuscular junction: resolution of a paradox. *J. Physiol. (Lond.)*. 251:245–270.
7. Magleby, K. L., and D. A. Terrar. 1975. Factors affecting the time course of decay of end-plate currents: a possible co-operative action of acetylcholine on receptors at the frog neuromuscular junction. *J. Physiol. (Lond.)*. 244:467–496.
8. Ruff, R. L. 1976. Local anesthetic alteration of miniature end-plate currents and end-plate current fluctuations. *Biophys. J.* 16:433–439.
9. Ruff, R. L. 1977. A quantitative analysis of local anesthetic alteration of miniature end-plate currents and end-plate current fluctuations. *J. Physiol. (Lond.)*. 264:89–124.
10. Neher, E., and B. Sakmann. 1976. Single-channel currents recorded from membrane of denervated frog muscle fibers. *Nature (Lond.)*. 260:799–802.
11. Magleby, K. L., and C. F. Stevens. 1972. A quantitative description of end-plate currents. *J. Physiol. (Lond.)*. 223:173–197.
12. Gage, P. W., and C. M. Armstrong. 1968. Miniature end-plate currents in voltage clamped muscular fibers. *Nature (Lond.)*. 218:363–365.
13. Steinbach, A. B. 1968. Alteration of xylocaine (lidocaine) and its derivatives of time-course of the end-plate potential. *J. Gen. Physiol.* 52:144–161.
14. Kordas, M. 1970. The effect of procaine on neuromuscular transmission. *J. Physiol. (Lond.)*. 209:689–699.
15. Deguchi, T., and T. Narahasi. 1971. Effects of procaine on ionic conductances of end-plate membranes. *J. Pharmac. Exp. Ther.* 176:423–433.
16. Maeno, T., C. Edwards, and S. Hashimura. 1971. Difference in effects on end-plate potentials between procaine and lidocaine as revealed by voltage-clamp experiments. *J. Neurophysiol.* 34:32–46.
17. Beam, K. G. 1976. A voltage clamp study of the effect of two lidocaine derivatives on the time course of end-plate currents. *J. Physiol. (Lond.)*. 258:279–300.
18. Adams, P. R. 1977. Voltage jump analysis of procaine action at frog end-plate. *J. Physiol. (Lond.)*. 268:291–318.
19. Neher, E., and J. H. Steinbach. 1978. Local anesthetics transiently block currents through single acetylcholine receptors channels. *J. Physiol. (Lond.)*. 277:153–176.
20. Lewis, C. A. 1979. Ion-concentration dependence of the reversal potential and the single channel conductance of ion channels at the frog neuromuscular junction. *J. Physiol. (Lond.)*. 286:417–445.
21. Lewis, C. A., and C. F. Stevens. 1979. Mechanisms of ion permeation through channels in a post-synaptic membrane. *In* Membrane Transport Processes. C. F. Stevens and R. W. Tsien, editors. Raven Press, New York. 133–151.
22. Dwyer, T. A., D. J. Adams, and B. Hille. 1980. The permeability of the end-plate channel to organic cation in frog muscle. *J. Gen. Physiol.* 75:469–492.
23. Adams, D. J., T. M. Dwyer, and B. Hille. 1980. The permeability of end-plate channels to monovalent and divalent metal cations. *J. Gen. Physiol.* 75:493–510.
24. Katz, B., and R. Miledi. 1972. The statistical nature of the acetyl-

choline potential and its molecular components. *J. Physiol. (Lond.)*. 224:665–669.
25. Neher, E., and B. Sakmann. 1976. Noise analysis of drug induced voltage clamp currents in denervated frog muscle fibres. *J. Physiol. (Lond.)*. 258:705–729.
26. Gage, P. W., and O. P. Hamill. 1980. Lifetime and conductance of acetylcholine-activated channels in normal and denervated toad sartorius muscle. *J. Physiol. (Lond.)*. 298:525–538.
27. Colquhoun, D., V. Dionne, J. H. Steinbach, and C. F. Stevens. 1975. Conductance of channels opened by acetylcholine-like drugs in the muscle end-plate. *Nature (Lond.)*. 253:204–206.
28. Beam, K. G. 1975. A quantitative description of end-plate currents in the presence of two lidocaine derivatives. *J. Physiol. (Lond.)*. 258:301–322.
29. Steinbach, A. B. 1968. A kinetic model for the action of xylocaine on receptors for acetylcholine. *J. Gen. Physiol.* 52:162–180.
30. Redmann, G. A. 1980. Local anesthetic block of the end-plate channel in high external sodium. *Soc. Neurosci. Abstr.* 6:778.
31. Adams, P. R. 1976. Drug blockade of open end-plate channels. *J. Physiol. Lond.* 260:531–552.
32. Adams, P. R., and B. Sakmann. 1978. Decamethonium both opens and blocks end-plate channels. *Proc. Natl. Acad. Sci.* 75:2994–2998.
33. Adams, P. R., and A. Feltz. 1980. Quinacrine (mepacrine) action at frog end-plate. *J. Physiol. (Lond.)*. 306:261–281.
34. Adams, P. R., and A. Feltz. 1980. End-plate channel opening and the kinetics of quinacrine (mepacrine) block. *J. Physiol. (Lond.)*. 306:283–306.
35. Hille, B. 1977. Local anesthetics: hydrophiloc and hydrophobic pathways for the drug receptor reaction. *J. Gen. Physiol.* 69:497–515.
36. Marty, A. 1978. Noise and relaxation studies of acetylcholine induced currents in the presence of procaine. *J. Physiol. (Lond.)*. 278:237–250.
37. Woodhull, A. M. 1973. Ionic blockages of sodium channels in nerve. *J. Gen. Physiol.* 61:687–708.
38. Katz, B., and R. Miledi. 1975. The effect of procaine on the action of acetylcholine at the neuromuscular junction. *J. Physiol. (Lond.)*. 249:269–284.